Peptidyl Aldehydes as Reversible Covalent Inhibitors of Protein Tyrosine Phosphatases†

Hua Fu,‡ Junguk Park,‡ and Dehua Pei*

Department of Chemistry and Ohio State Biochemistry Program, The Ohio State University, 100 West 18th Avenue, Columbus, Ohio 43210

Received March 26, 2002; Revised Manuscript Received June 1, 2002

ABSTRACT: Protein tyrosine phosphatases (PTPs) are a large family of enzymes that catalyze the hydrolytic removal of the phosphoryl group from phosphotyrosyl (pY) proteins. PTP inhibitors provide potential treatment of human diseases/conditions such as diabetes and obesity as well as useful tools for studying the function of PTPs in signaling pathways. In this work, we have shown that certain aryl-substituted aldehydes act as reversible, slow-binding inhibitors of modest potency against PTP1B, SHP-1, and a dual-specificity phosphatase, VHR. Attachment of the tripeptide Gly-Glu-Glu to the para position of cinnamaldehyde resulted in an inhibitor (Cinn-GEE) of substantially increased potency against all three enzymes (e.g., $K_I^* = 5.4\ \mu M$ against PTP1B). The mechanism of inhibition was investigated using Cinn-GEE specifically labeled with ^{13}C at the aldehyde carbon and ^{1}H-^{13}C heteronuclear single-quantum coherence spectroscopy. While Cinn-GEE alone showed a single cross-peak at δ 9.64 (^{1}H) and δ 201 (^{13}C), the PTP1B/Cinn-GEE complex showed three distinct cross-peaks at δ 7.6−7.8 (^{1}H) and 130−137 (^{13}C). Mutation of the catalytic cysteine (Cys-215 in PTP1B) into alanine had no effect on the cross-peaks, whereas mutation of a conserved active-site arginine (Arg-221 in PTP1B) to alanine abolished all three cross-peaks. Similar experiments with Cinn-GEE that had been labeled with ^{13}C at the benzylic position revealed a change in the hybridization state (from sp^2 to sp^3) for the benzylic carbon as a result of binding to PTP1B. These results rule out the possibility of a free aldehyde, aldehyde hydrate, or hemithioacetal as the enzyme-bound inhibitor form. Instead, the data are consistent with the formation of an enamine between the aldehyde group of the inhibitor and the guanidine group of Arg-221 in the PTP1B active site. These aldehydes may provide a general core structure that can be further developed into highly potent and specific PTP inhibitors.

Protein tyrosine phosphatases (PTPs)[1] are a diverse family of enzymes that catalyze the hydrolysis of phosphotyrosine (pY) residues in proteins. These enzymes, together with the protein tyrosine kinases (PTKs), control the level of intracellular tyrosine phosphorylation, thus regulating many cellular functions (*1*). The malfunction of either PTKs or PTPs can lead to a variety of human diseases and conditions (*2*, *3*). Therefore, inhibitors against these signaling molecules provide potential therapeutic agents. For example, a great deal of effort is currently being made by both academic and industrial labs to develop specific inhibitors for PTP1B, which has been shown to be a promising target for the treatment of type II diabetes (*4*). Specific PTK and PTP inhibitors would also be very useful probes for studying the physiological functions of these enzymes. To date, a large number of PTKs and PTPs have been identified, but their precise mechanisms of action in vivo are largely unknown.

A variety of PTP inhibitors have been reported in recent years (reviewed in *5*). Virtually all of these inhibitors contain a nonhydrolyzable pY mimetic, such as phosphonates (*6*−*10*), malonates (*11*−*14*), aryl carboxylates (*15*−*19*), or cinnamates (*20*, *21*), as the inhibitor core structure. A common feature of these inhibitors is that they all carry at least one negative charge, which may impede their membrane permeability. Therefore, although some of these inhibitors have shown impressive potency in vitro (*10*, *19*, *20*), their application as therapeutic agents or research tools in whole cell assays has yet to be realized. A few natural (*22*, *23*) and synthetic products (*24*) have also been found to show inhibitory activity toward PTPs, but they are generally weak inhibitors.

Our laboratory has been undertaking an alternative approach to designing PTP inhibitors by covalently modifying its conserved active-site residues. All of the known PTPs contain an invariant sequence motif at the active site, (I/V)-$HC(X)_5R(S/T)$, where the cysteine and arginine residues are strictly conserved. Mechanistically, the cysteine thiol is the catalytic nucleophile, which attacks the phosphate of pY to form a transient phosphocysteinyl enzyme intermediate (*25*).

† This work was supported in part by a grant from the National Institutes of Health (AI40575).

* To whom correspondence should be addressed at the Department of Chemistry, The Ohio State University, 100 W. 18th Ave., Columbus, OH 43210. Telephone: (614) 688-4068. Fax: (614) 292-1532. E-mail: pei.3@osu.edu.

‡ These two authors contributed equally to this work.

[1] Abbreviations: Cinn-GEE, *N*-[4-(3-oxo-1-propenyl)benzoyl]-Gly-Glu-Glu-NH_2; PTP, protein tyrosine phosphatase; PTK, protein tyrosine kinase; pY, phosphotyrosine; *p*NPP, *p*-nitrophenyl phosphate.

10.1021/bi0258748 CCC: $22.00
Published on Web 08/03/2002

The arginine is critical for both substrate binding and stabilization of the transition state by neutralizing the developing negative charge on the phosphate group (*26*). Mutation or chemical modification of the active-site cysteine results in total loss of activity (*27*, *28*), whereas removal of the arginine side chain reduces the activity by $>10^4$-fold (*26*). We have previously demonstrated that α-haloacetophenone derivatives act as potent, time-dependent inactivators of PTPs by alkylating the active-site cysteine (*29*). We now report that simple aldehydes act as slow-binding, reversible inhibitors of PTPs by forming an imine/enamine adduct with the active-site arginine.

MATERIALS AND METHODS

Materials and General Methods. The catalytic domain of SHP-1, SHP-1(ΔSH2), was purified from a recombinant *Escherichia coli* strain as previously described (*30*). The catalytic domain of PTP1B (residues 1−321) and VHR were expressed in *E. coli* and purified to near-homogeneity according to literature procedures (*31*, *32*). PTP1B mutants (C215A and R221A) were generated by the Quick-Change mutagenesis method (Stratagene). The entire coding region was sequenced to ensure the presence of the desired mutations as well as the absence of any undesired mutations. All of the peptide synthesis reagents were purchased from Advanced ChemTech (Louisville, KY). The Rink resin had a loading capacity of 0.7 mmol/g. All other chemicals were obtained from Aldrich or Sigma.

*Methyl 4-[2-(1,3-Dioxolane-2-yl)-ethenyl]benzoate (**6**)*. This compound was prepared by modification of a literature procedure (*33*). Methyl 4-formylbenzoate (0.82 g, 5.0 mmol) and tris(methoxyethoxyethyl)amine (TMA) (1.62 g, 5.0 mmol) were dissolved in 30 mL of dichloromethane under argon at room temperature. A saturated aqueous K_2CO_3 solution (30 mL) and (1,3-dioxolane-2-yl-methyl)triphenylphosphonium bromide (2.15 g, 5 mmol) were added, and the reaction mixture was refluxed (∼40 °C) for 16 h with vigorous stirring. The reaction product was extracted into dichloromethane (3 × 20 mL), washed with water (20 mL), and dried over $MgSO_4$. Compound **6** was obtained as a 67:33 mixture of *Z* and *E* isomers after chromatography on a silica gel column (6:1 hexane/ethyl acetate) (yield: 1.16 g, 99.1%). ^{1}H NMR (250 MHz, $CDCl_3$) δ 7.97−8.10 (m, 2H, Ar), 7.52−7.76 (m, 2H, Ar), 6.83−6.93 (m, 1H, ArC*H*═CHCH), 6.36 (dd, 0.33H, ArCH═C*H*CH *E*, *J* = 5.8 Hz, 16.1 Hz), 5.81 (dd, 0.67H, ArCH═C*H*CH *Z*, *J* = 7.4 Hz, 11.8 Hz), 5.45 (d, 0.67H, ArCH═CHC*H Z*, *J* = 7.4 Hz), 5.39 (d, 0.33H, ArCH═CHC*H E*, *J* = 5.9 Hz), 3.88−4.18 (m, 7H, CH_3, OCH_2CH_2O); ^{13}C NMR (62.5 MHz, $CDCl_3$) δ 166.63, 141.31, 134.39, 133.47, 131.39, 130.58, 130.13, 129.83, 127.64, 104.06, 99.98, 65.76, 65.61, 52.31.

*Methyl 4-(3-Oxo-1-propenyl)benzoate (**9**)*. Compound **6** (0.12 g, 0.5 mmol) was added to 5 mL of 90% aqueous TFA, and the solution was stirred for 1 h. After removal of solvents by rotary evaporation, the residue was dried over P_2O_5 in vacuo to a white solid as pure *E* isomer (95 mg, quantitative yield). ^{1}H NMR (250 MHz, $CDCl_3$) δ 9.74 (d, 1H, C*H*O, *J* = 7.5 Hz), 8.09 (d, 2H, Ar, *J* = 8.4 Hz), 7.87 (d, 2H, Ar, *J* = 8.4 Hz), 7.77 (d, 1H, ArC*H*═CHCH, *J* = 16.1 Hz), 6.87 (dd, 1H, ArCH═C*H*CH, *J* = 7.5 Hz, 13.3 Hz), 3.91 (s, 3H, OCH_3); ^{13}C NMR (62.5 MHz, $CDCl_3$) δ 194.12, 166.61, 151.62, 132.86, 131.44, 129.47, 52.59.

*4-(3-Oxo-1-propenyl)benzoic Acid (**3**)*. Compound **9** (48 mg) was added to 3 mL of an aqueous NaOH solution (40 mg, 1 mmol), and the solution was stirred overnight at room temperature. After removal of methanol by rotary evaporation, the remaining solution was diluted with 5 mL of H_2O and acidified to pH 2 with HCl. The solution was extracted with ethyl acetate (3 × 10 mL), and the combined organic phase was dried over $MgSO_4$. Evaporation of solvent afforded 41 mg of a light yellow solid (92.4% yield). ^{1}H NMR (250 MHz, $CDCl_3$) δ 10.46 (s, 1H, COO*H*), 9.78 (d, 1H, C*H*O, *J* = 7.6 Hz), 8.14 (d, 2H, Ar, *J* = 8.3 Hz), 7.88 (d, 2H, Ar, *J* = 8.3 Hz), 7.78 (d, 1H, ArC*H*═CHCH, *J* = 16.1 Hz), 6.89 (dd, 1H, ArCH═C*H*CH, *J* = 7.5 Hz, 16.0 Hz); ^{13}C NMR (62.5 MHz, $CDCl_3$) δ 194.15, 164.15, 151.24, 134.52, 131.07, 129.45.

*Ethyl 4-[2-(1,3-Dioxolane-2-yl)-ethenyl]benzoyl Carbonate (**7**)*. An aqueous NaOH solution (0.8 g dissolved in 8 mL of H_2O) was added to compound **6** (1.16 g, 5.0 mmol) dissolved in 8 mL of methanol. The solution was stirred for 16 h at room temperature, followed by solvent evaporation. The solid residue was dried over P_2O_5 in vacuo to produce the corresponding sodium salt, which was stable during storage in a −5 °C freezer. Ethyl chloroformate (0.26 g, 24 mmol) was added to a 15 mL suspension of the salt (0.14 g) in CH_2Cl_2 under argon, and the mixture was stirred for 2 h at room temperature and filtered. The filtrate was evaporated under reduced pressure to obtain 0.12 g of an oil (isomer *Z*:*E* = 62:38) (86% yield). ^{1}H NMR (250 MHz, $CDCl_3$) δ 8.02−8.08 (m, 2H, Ar), 7.60−7.72 (m, 2H, Ar), 6.86−6.92 (m, 1H, ArC*H*═CHCH), 6.42 (dd, 0.38H, ArCH═C*H*CH *E*, *J* = 5.8 Hz, 16.1 Hz), 5.86 (dd, 0.62H, ArCH═C*H*CH *Z*, *J* = 7.4 Hz, 11.8 Hz), 5.46 (d, 0.62H, ArCH═CHC*H Z*, *J* = 7.4 Hz), 5.41 (d, 0.38H, ArCH═CHC*H E*, *J* = 5.9 Hz), 4.29−4.42 (m, 2H, CH_2CH$_3$), 3.91−3.94 (m, 4H, OCH_2CH_2O), 1.29−1.38 (m, 3H, CH$_2$CH_3); ^{13}C NMR (62.5 MHz, $CDCl_3$) δ 161.80, 149.93, 149.30, 143.33, 143.09, 134.00, 132.24, 131.57, 131.28, 131.11, 130.99, 130.39, 128.19, 127.85, 127.57, 103.85, 99.85, 66.71, 65.79, 65.63, 14.15.

*N-[4-(3-Oxo-1-propenyl)benzoyl]-Gly-Glu-Glu-NH$_2$ (**5**)*. The tripeptide Gly-Glu-Glu was synthesized on 0.18 g of Rink resin (0.11 mmol) using standard Fmoc/HBTU/HOBt solid-phase peptide chemistry. Next, 61.3 mg (0.21 mmol) of anhydride **7** in 2.5 mL of CH_2Cl_2 and 100 μL of *N*-methylmorpholine were added to the resin suspended in 2.5 mL of anhydrous DMF. The mixture was shaken for 8 h at room temperature. Ninhydrin tests indicated complete acylation of the N-terminal amine. The solvents were drained, and the resin was washed with DMF (5 × 5 mL) and CH_3-OH (3 × 5 mL). Deprotection of side-chain as well as aldehyde protecting groups and cleavage from the resin were carried out with a cocktail containing 4 mL of 90% TFA in water, 0.1 mL of anisole, and 0.15 mL of thioanisole for 3 h at room temperature. TFA, H_2O, and other volatile chemicals were removed under a gentle flow of nitrogen, and the residue was triturated 5 times with diethyl ether. Compound **5** was obtained as a brownish solid in the pure *E* isomer form (yield 48 mg). ^{1}H NMR (250 MHz, D_2O): 9.62 (d, C*H*O, *J* = 7.4 Hz), 7.79−7.86 (m, Ar, ArC*H*═CHCH), 6.87 (dd, ArCH═C*H*CH, *J* = 7.5 Hz, 16.0 Hz),

4.11−4.42 (m, α-CH of Glu), 3.84 (s, α-CH_2 of Gly), 2.37−2.42 (m, 2 CH_2CH_2COOH), 1.96−2.12 (m, 2 CH_2CH_2-COOH). HRESI-MS: $C_{22}H_{26}O_9N_4Na^+$ ($[M+Na]^+$), calcd 513.1592, found 513.1576.

*Methyl 4-(3-[^{13}C]Oxo-1-propenyl)benzoate (**10**).* (Triphenylphosphoranylidene)-[1-^{13}C]acetaldehyde (**11**) was synthesized as previously described (*34*). The crude aldehyde **11** (0.85 g, 2.8 mmol) after crystallization was dissolved in 25 mL of benzene and mixed with methyl 4-formyl benzoate (0.7 g, 4.3 mmol). The solution was stirred for 6 h at room temperature, and the solvent was removed by rotary evaporation. Chromatography on a silica gel column (hexane/ethyl acetate = 6:1) afforded 0.17 g of a white solid (26% yield for two steps). ^{1}H NMR (250 MHz, $CDCl_3$): δ 9.75 (dd, 1H, ^{13}CHO, $^3J_{H-H}$ = 7.6 Hz, $^1J_{C-H}$ = 173.1 Hz), 8.09 (d, 2H, Ar, $^3J_{H-H}$ = 6.7 Hz), 7.64 (d, 2H, Ar, $^3J_{H-H}$ = 8.4 Hz), 7.50 (d, 1H, ArC*H*=CHCH, $^3J_{H-H}$ = 16.0 Hz, $^3J_{C-H}$ = 33.5 Hz), 6.78 (ddd, 1H, ArCH=C*H*CH *E*, $^3J_{H-H}$ = 7.5 Hz, 16.0 Hz, $^2J_{C-H}$ = 0.85 Hz), 3.95 (s, 3H, OCH_3); ^{13}C NMR (62.5 MHz, $CDCl_3$) δ 193.65.

*Methyl 4-[2-(1,3-Dioxolane-2-[^{13}C]yl)-ethenyl]benzoate (**12**).* A solution of ethylene glycol (0.11 g, 1.78 mmol) in benzene (5 mL) was added to a round-bottomed flask containing compound **10** (0.17 g, 0.89 mmol), *p*-toluenesulfonic acid monohydrate (3 mg), $MgSO_4$ (0.22 g, 1.78 mmol), and benzene (25 mL). The reaction mixture was heated to reflux for 8 h. After cooling, solid $NaHCO_3$ (5.4 mg, 0.064 mmol) was added to the mixture to neutralize the *p*-toluenesulfonic acid, and the mixture was stirred for 30 min. The reaction mixture was then filtered through a pad of anhydrous $NaHCO_3$, and the filter cake was washed with CH_2Cl_2 (3 × 10 mL). The filtrate was concentrated and purified by flash column chromatography on a silica gel column (6:1 hexane/ethyl acetate) to obtain 0.14 g of a white solid (67% yield). ^{1}H NMR (250 MHz, $CDCl_3$) δ 7.99 (d, 2H, Ar, $^3J_{H-H}$ = 6.6 Hz), 7.63 (d, 2H, Ar, $^3J_{H-H}$ = 6.6 Hz,), 6.87 (dd, 1H, ArC*H*=CHCH, $^3J_{H-H}$ = 16.0 Hz, $^3J_{C-H}$ = 6.7 Hz), 6.37 (dd, 1H, ArCH=C*H*CH *E*, $^3J_{H-H}$ = 5.8 Hz, 16.0 Hz), 5.39 (dd, 1H, $^3J_{H-H}$ = 5.9 Hz, $^2J_{C-H}$ = 167.43 Hz), 3.88−4.04 (m, 7H, OCH_3, OCH_2CH_2O); ^{13}C NMR (62.5 MHz, $CDCl_3$) δ 104.08.

*Ethyl 4-[2-(1,3-Dioxolane-2-[^{13}C]yl)-ethenyl]benzoyl Carbonate (**13**).* This was prepared as described for **7**. ^{1}H NMR (250 MHz, $CDCl_3$) δ 8.03 (d, 2H, Ar, $^3J_{H-H}$ = 8.0 Hz), 7.51 (d, 2H, Ar, $^3J_{H-H}$ = 8.05 Hz), 6.82 (dd, 1H, ArC*H*=CHCH, $^3J_{H-H}$ = 15.8 Hz, $^3J_{C-H}$ = 7.45 Hz), 6.31 (dd, 1H, ArCH=C*H*CH *E*, $^3J_{H-H}$ = 5.6 Hz, 15.9 Hz), 5.46 (dd, 1H, $^3J_{H-H}$ = 5.6 Hz, $^2J_{C-H}$ = 168.1 Hz), 4.40 (m, 2H, OCH_2CH_3), 3.96−4.09 (m, 4H, OCH_2CH_2O), 1.44 (t, 3H, OCH_2CH_3); ^{13}C NMR (62.5 MHz, $CDCl_3$) δ 103.52.

*N-[4-(3-[^{13}C]Oxo-1-propenyl)benzoyl]-Gly-Glu-Glu-NH_2 (**14**).* This was prepared from anhydride **13** in a manner similar to **5**. ^{13}C NMR (62.5 MHz, $CDCl_3$) δ 194.43.

*Methyl 4-[^{13}C]Cyanobenzoate (**15**).* This compound was synthesized from [^{13}C]KCN according to a literature procedure (Scheme 3) (*35*). ^{1}H NMR (250 MHz, $CDCl_3$) δ 8.13 (d, 2H, Ar, J = 8.2 Hz), 7.80 (d, 2H, Ar, J = 8.2 Hz), 3.95 (s, 3H, OCH_3); ^{13}C NMR (62.5 MHz, $CDCl_3$) δ 118.35.

*Methyl 4-[^{13}C]Formyl Benzoate (**16**).* Nickel/aluminum alloy (1:1 w/w, 80 mg) was added to methyl 4-[^{13}C]-cyanobenzoate **15** (640 mg, 3.95 mmol) in aqueous formic acid [10 mL, 3:1 formic acid/water (v/v)]. The suspension was refluxed for 1 h, cooled, and filtered, and the residual alloy was rinsed with ethanol (2 mL), chloroform (4 mL), and diethyl ether (5 mL). The filtrate was extracted with chloroform (2 × 20 mL). The organic phase was washed with water (15 mL) and then a saturated sodium bicarbonate solution (15 mL). The water and sodium bicarbonate phases were back-extracted with chloroform (10 mL) and then diethyl ether (10 mL). The combined organic phase was dried over anhydrous magnesium sulfate and evaporated in vacuo to yield 0.53 g of a semisolid (81% yield), which was used without further purification. ^{1}H NMR (250 MHz, $CDCl_3$) δ 10.08 (d, 1H, *C*H*O, J = 162.5 Hz), 8.18 (d, 2H, Ar, J = 8.3 Hz), 7.96 (d, 2H, Ar, J = 8.23 Hz), 3.94 (s, 3H, OCH_3); ^{13}C NMR (62.5 MHz, $CDCl_3$) δ 191.88.

*N-[4-(3-Oxo-1-[^{13}C]propenyl)benzoyl]-Gly-Glu-Glu-NH_2 (**17**).* This was prepared from aldehyde **16** in a manner similar to **5**. ^{13}C NMR (62.5 MHz, $CDCl_3$) δ 152.16.

PTP Inhibition Assays. Stock solutions of inhibitors were prepared in dimethyl sulfoxide (DMSO), and their concentrations were calculated from the known inhibitor masses and solvent volumes. A typical reaction (total volume 1 mL) contained 50 mM HEPES (pH 7.4), 1 mM EDTA, 1 mM tris(carboxyethyl)phosphine (TCEP), 50 mM NaCl, 5% (v/v) DMSO, 0.1−0.2 μM PTP, and 0−2000 μM inhibitor. After incubation of the enzyme with the inhibitor for 1 h at room temperature, the reaction was initiated by the addition of 1.0 mM *p*-nitrophenyl phosphate (*p*NPP). The reaction progress was monitored at 405 nm on a Perkin-Ellmer UV−Vis spectrophotometer. The IC_{50} values were determined by plotting the remaining activity as a function of inhibitor concentration, and the K_I* values were obtained by fitting the data to the Michaelis−Menten equation. To determine the K_I value, the reaction was initiated by addition of enzyme (0.2 μM) into the above reaction mixture, which also contained 1.0 mM *p*NPP. The reaction was monitored continuously on the UV−Vis spectrophotometer, and the initial reaction rates (<15 s) were fitted to the Michaelis−Menten equation.

To determine the rate constant k_6, the enzyme (1.0 μM) was incubated with 50−100 μM inhibitor in 100 μL of the above reaction buffer for 3 h at room temperature. The mixture was rapidly diluted into 900 μL of the same reaction buffer containing 1.0 mM *p*NPP (without inhibitor). Reactivation of PTP activity was monitored at 405 nm, and the progress curves were fit to the equation:

$$\mathrm{Abs}_{405} = v_s[t - (1 - e^{-k_6 t})/k_6]$$

where v_s is the final steady-state velocity. The rate constant k_5 was calculated using the equation: $K_I^* = K_I k_6/(k_5 + k_6)$.

Inactivation of Inhibitor Cinn-GEE by Cysteamine. Cinn-GEE (1 mM) was incubated with 100 mM cysteamine hydrochloride (which had been neutralized by the addition of 1.0 equiv of NaOH) in 100 μL of a 97:3 DMSO/H_2O mixture for 24 h. The treated inhibitor was then used in inhibition assays as described above. As a control, inhibition assay was also performed with the same amount of cysteamine hydrochloride/NaOH solution.

NMR Spectroscopy of [^{13}C]Cinn-GEE and [^{13}C]Cinn-GEE−PTP1B Complex. All NMR experiments were

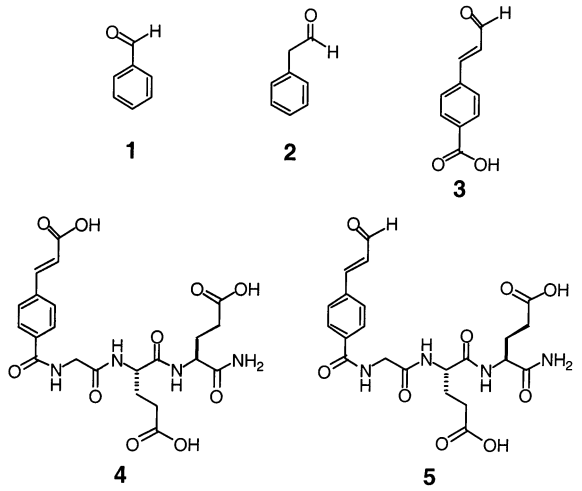

FIGURE 1: Structures of PTP inhibitors.

performed on a Bruker DMX-600 NMR spectrometer equipped with a triple-resonance and 3-axis gradient probe at 300 K. The 2D ^{1}H-^{13}C heteronuclear single-quantum coherence spectra (HSQC) were acquired using a constant-time sensitivity-enhanced method (*36*, *37*). All samples were dissolved in a buffer containing 5 mM Hepes (pH 7.4), 150 mM NaCl, 5 mM EDTA, and 2 mM β-mercaptoethanol (94:6 H_2O/D_2O). The spectral widths were 9615 Hz in the ^{1}H dimension and 19 621 Hz in the ^{13}C dimension, with carrier frequencies at 4.7 and 150 ppm (for ^{13}C at the aldehyde position) or 100 ppm (for ^{13}C at the benzylic position), respectively.

RESULTS

Inhibition of PTPs by Simple Aldehydes. Peptidyl aldehydes represent an important class of inhibitors for cysteine proteases which, like PTPs, also utilize an active-site cysteine as the catalytic nucleophile (*38*). These aldehydes bind to the proteases through the formation of a covalent but reversible hemithioacetal adduct with the active-site cysteine. Calpeptin, a potent dipeptide aldehyde inhibitor of calpain, has recently been reported to show modest cross-reactivity toward several PTPs (*39*, *40*). These observations led us to hypothesize that aryl-substituted aldehydes might serve as selective PTP inhibitors. We therefore tested several aryl aldehydes (Figure 1) against tyrosine phosphatases PTP1B and SHP-1, and a dual-specificity phosphatase, VHR. 4-Carboxycinnamaldehyde (**3**) was the most active against PTPs among the three aldehydes tested, with IC_{50} values of 230 and 970 μM against SHP-1 and PTP1B, respectively (Figure 2 and Table 1). It showed no significant inhibition against VHR up to 2 mM. Benzaldehyde was the least active inhibitor against all PTPs, presumably because its carbonyl group cannot readily reach the nucleophile(s) in the deep active-site pocket. All of the inhibitors were less active against VHR, which has a wider, shallower active-site pocket as compared to PTPs (*41*). Due to limited solubility, the IC_{50} values for some enzyme/inhibitor pairs could not be determined.

Slow-Binding Inhibition of PTPs by Cinn-GEE. The simple aldehydes presumably interact with only the active-site pocket of PTPs, limiting their inhibitory potency. One approach to improving their potency is to modify the

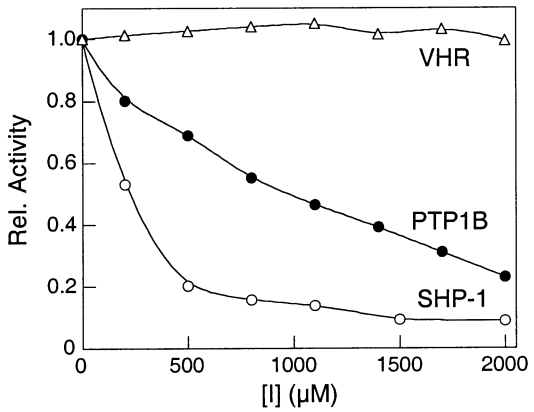

FIGURE 2: Plot of remaining PTP activity against inhibitor **3** concentration. All of the activities are relative to those in the absence of inhibitor.

Table 1: Inhibitory Activity of Aldehydes against Various PTPs

	inhibition constant (IC_{50} or K_I*, μM)		
inhibitor	PTP1B	SHP-1	VHR
1	NA	NA	NA
2	15% (at 200 μM)	NA	NA
3	970[a]	230[a]	>2000[a]
4	0.079[b]		
5	5.42 ± 0.94[c]	10.7 ± 1.4[c]	288 ± 112[c]

[a] IC_{50} values. [b] K_I value from Moran et al. (*20*). [c] K_I* values; NA, no significant activity.

aldehydes with functional groups that can interact with the protein surfaces near the active site. These additional interactions would also confer selectivity for a particular PTP on the inhibitor. Moran et al. have shown that attachment of a tripeptide, Gly-Glu-Glu-NH_2 (GEE), to the para position of cinnamic acid results in a potent inhibitor (compound **4**) for PTP1B (K_I = 79 nM), although cinnamic acid alone shows only weak activity (*20*). As a proof of principle, we attached the tripeptide GEE to the para position of cinnamaldehyde to obtain *N*-[4-(3-oxo-1-propenyl)benzoyl]-Gly-Glu-Glu-NH_2 (Cinn-GEE) (compound **5** in Figure 1). Cinn-GEE was synthesized from commercially available materials as detailed under Materials and Methods (Scheme 1).

Cinn-GEE exhibited time-dependent inhibition toward PTP1B, SHP-1, and VHR. It resulted in biphasic curves when the hydrolysis of *p*NPP by PTPs was monitored in a continuous fashion, indicative of slow-binding inhibition (Figure 3A) (*42*). The inhibition kinetics can be described by the equation:

$$E + I \overset{K_I}{\rightleftharpoons} E\cdot I \underset{k_6}{\overset{k_5}{\rightleftharpoons}} E\cdot I^*$$

where K_I is the equilibrium inhibition constant for the formation of the initial complex, E·I, and k_5 and k_6 are the forward and reverse rate constants for the slow conversion of the initial E·I complex into a tight complex E·I*, respectively. The overall potency of the inhibitor is described by the overall equilibrium constant, $K_I^* = K_I k_6/(k_5 + k_6)$. The K_I* values of Cinn-GEE were 5.4, 10.7, and 288 μM against PTP1B, SHP-1, and VHR, respectively (Table 1). To distinguish the observed slow-binding behavior from time-dependent inactivation, PTP1B was preincubated with excess Cinn-GEE to form the E·I* complex, which was then

Scheme 1

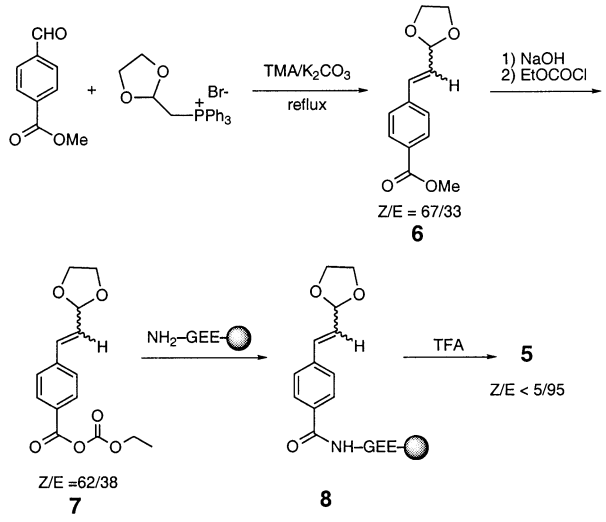

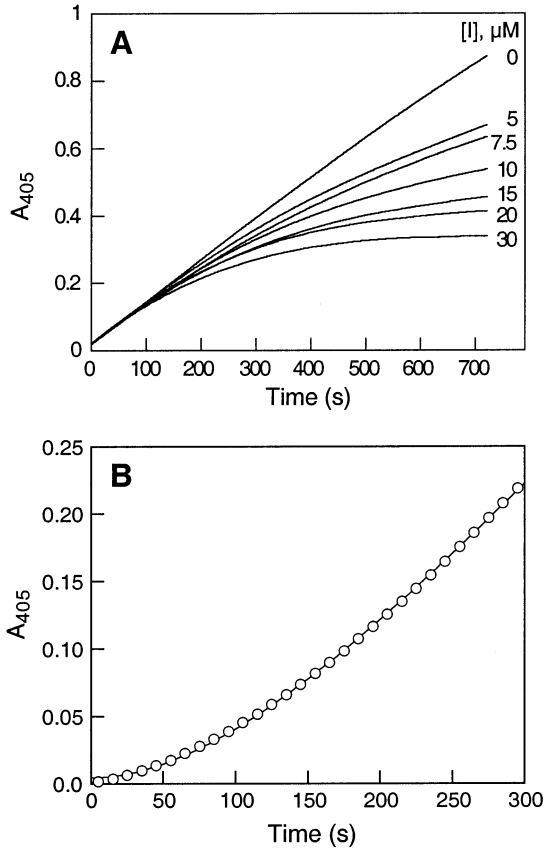

FIGURE 3: Slow-binding inhibition of PTP1B by Cinn-GEE. (A) Hydrolysis of *p*NPP (1.0 mM) by PTP1B (0.2 μM) in the presence of the indicated amounts of Cinn-GEE. The reactions were initiated by the addition of enzyme as the last component. (B) Hydrolysis of *p*NPP by reactivated PTP1B. The enzyme (1.0 μM) was preincubated with Cinn-GEE (75 μM) for 3 h before being diluted 10-fold into the reaction buffer containing 1.0 mM *p*NPP.

rapidly diluted into an assay solution containing *p*NPP as substrate. The reaction progress as a function of time is shown in Figure 3B. The slow reactivation of the enzyme with time is consistent with the slow-binding mechanism. Curve-fitting indicates that the rate for reactivation of PTP1B (k_6) is 0.56 min^{-1}. Based on the K_I value of 550 μM for Cinn-GEE binding to PTP1B, the rate for the conversion of noncovalent E·I complex to the covalent E−I complex was

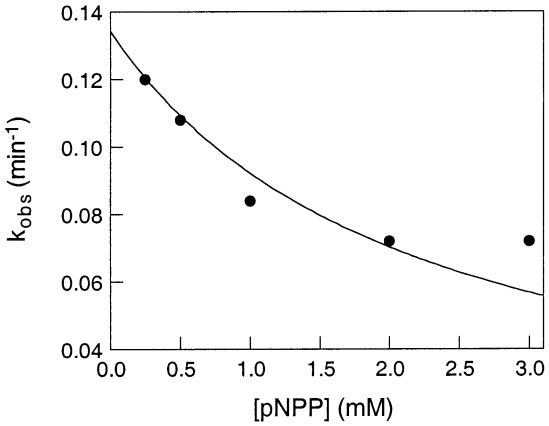

FIGURE 4: Competition between Cinn-GEE and substrate for binding to PTP1B. Reaction time courses were initiated by the addition of PTP1B (0.3 μM) to assay mixtures containing a fixed inhibitor concentration (40 μM) and varying *p*NPP concentration. The k_{obs} values were obtained from fitting individual times courses to the equation: $[P] = v_s t + [(v_i - v_s)/k_{obs}](1 - e^{-k_{obs}t})$. The solid line through the data is a best fit to the data according to equation: $k_{obs} = k_{max}/(1 + [pNPP]/K_M)$.

Scheme 2

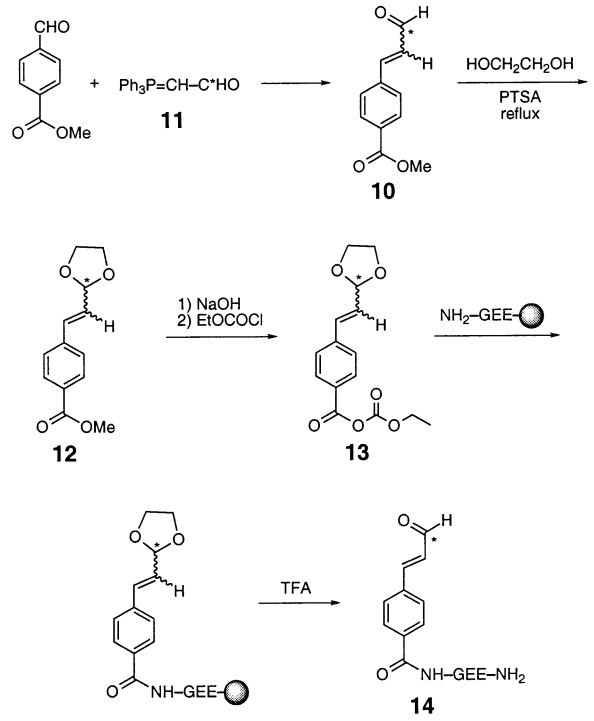

determined as 56 min^{-1}. 4-Carboxycinnamaldehyde exhibited similar slow-binding behavior toward the PTPs (data not shown), although the K_I, k_5, and k_6 values could not be reliably determined due to the weak binding affinity. The tripeptide (GEE-NH_2) alone did not inhibit any of the enzymes.

Cinn-GEE Is Active-Site-Directed. Competition with substrate was determined by measuring k_{obs}, the pseudo-first-order rate constant for onset of inhibition, from progress curves obtained at constant inhibitor but varying *p*NPP concentrations. Although the data are somewhat scattered due to technical difficulties in attaining final steady states in a reasonable time frame, there is clearly an inverse correlation between k_{obs} and *p*NPP concentration, as expected from competitive binding of Cinn-GEE and *p*NPP to the

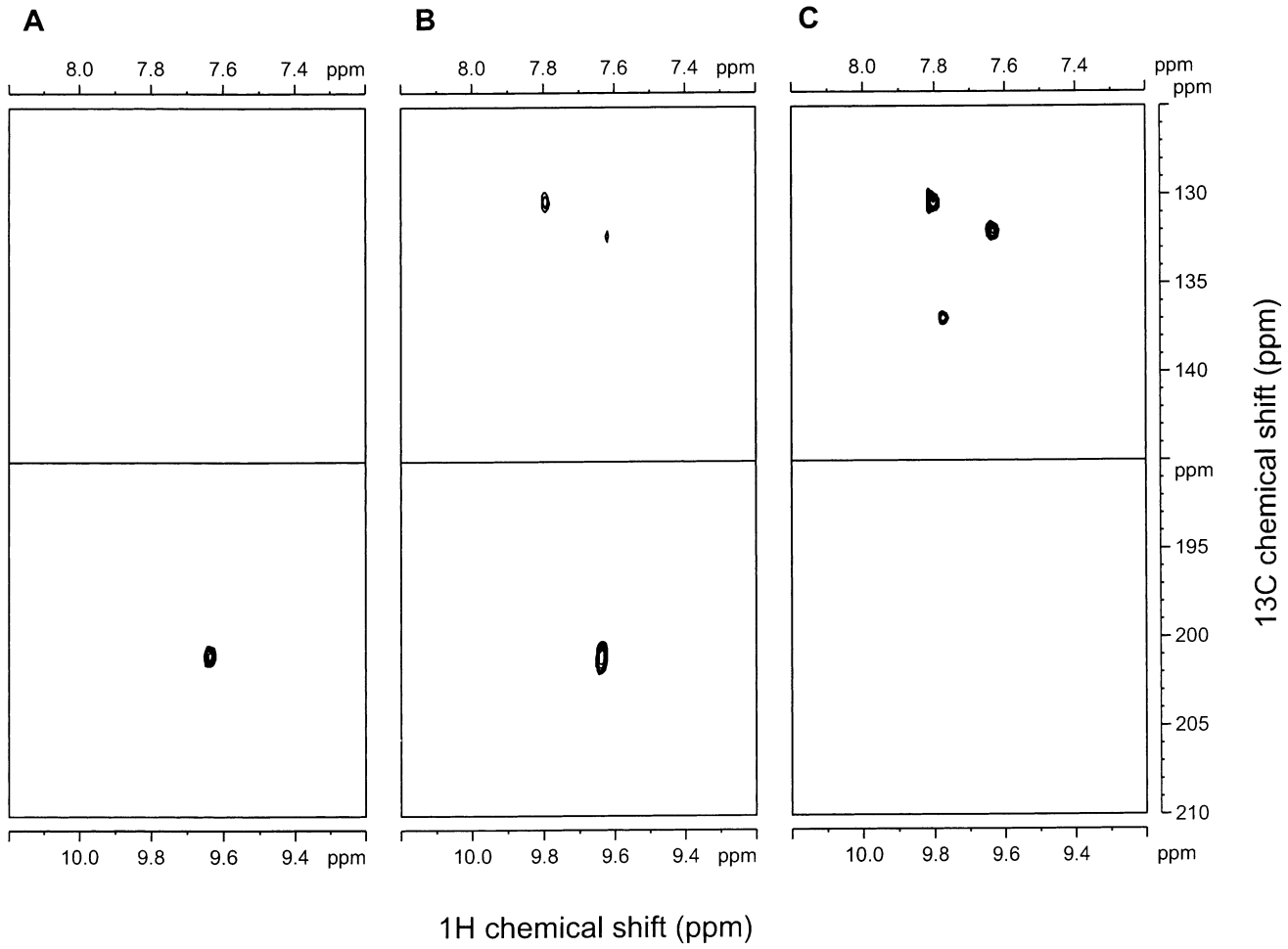

FIGURE 5: HSQC spectra of ^{13}C-labeled Cinn-GEE (compound **14**) in the presence and absence of PTP1B. (A) 200 μM Cinn-GEE only; (B) 200 μM Cinn-GEE and ~200 μM PTP1B; and (C) 200 μM Cinn-GEE and ~300 μM PTP1B. PTP1B concentration was based on the Bradford assay using bovine serum albumin as standard.

Scheme 3

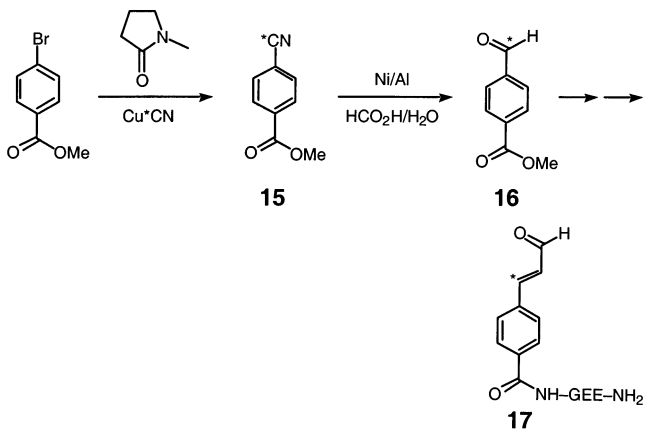

same active site (Figure 4). In another experiment (data not shown), PTP1B was first treated with a slight molar excess of *p*-hydroxyl α-bromoacetophenone, which inactivates PTPs by selectively alkylating the catalytic cysteine (*29*), and then examined for binding to Cinn-GEE by NMR spectroscopy (see below). Alkylation of the active-site cysteine abolished the ability of PTP1B to bind Cinn-GEE. These data strongly suggest that Cinn-GEE is active-sited-directed.

Mechanism of Inhibition. We initially hypothesized that the E·I complex was the noncovalent complex of PTP1B and Cinn-GEE, whereas the E·I* represented a covalent adduct formed between the inhibitor aldehyde and the thiol group of the enzyme active-site cysteine. To test this hypothesis, we synthesized Cinn-GEE labeled with ^{13}C at the aldehyde carbonyl carbon (Scheme 2, compound **14**) and analyzed both the inhibitor and the enzyme−inhibitor complex by ^{1}H-^{13}C HSQC NMR spectroscopy. When dissolved in the PTP assay buffer (pH 7.4), [^{13}C]Cinn-GEE alone showed a single cross-peak at δ 9.64 (^{1}H) and δ 201 (^{13}C) in the NMR spectrum (Figure 5A). This suggests that the free inhibitor existed predominantly in the aldehyde form in the aqueous solution. Upon addition of increasing concentrations of PTP1B (with preincubation), the signal of the free inhibitor decreased, with the concomitant appearance of two major peaks at δ 7.80/130 and δ 7.65/132, respectively, and a minor peak at δ 7.76/137 (Figure 5B). Finally, when PTP1B was added in excess, the free inhibitor signal was completely converted into the above three peaks (Figure 5C). No other signals were observed that could be attributed to either the free inhibitor or the enzyme−inhibitor complex. The same three peaks were also observed in the 1-D ^{13}C NMR spectrum of the PTP1B/Cinn-GEE complex (data not shown). These unexpected results (chemical shift values and the appearance of multiple peaks) are inconsistent with the formation of a hemithioacetal. On the basis of these observations, we proposed that the inhibitor aldehyde could react with the guanidine group of the catalytic arginine

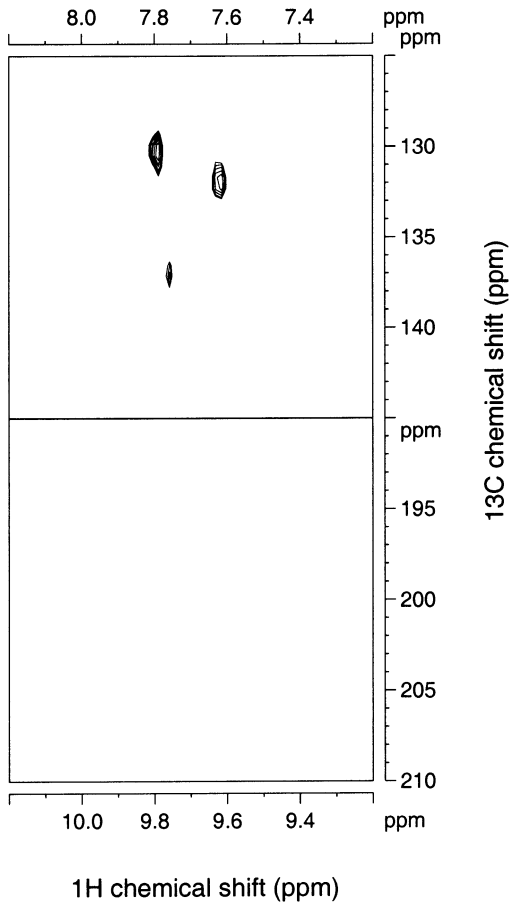

FIGURE 6: HSQC spectra of ^{13}C-labeled Cinn-GEE (compound **14**; 200 μM) in the presence of C215A PTP1B (500 μM).

residue (Arg-221 in PTP1B) to form an imine or enamine adduct.

To establish the role of Arg-221 in inhibitor binding, we performed the same HSQC experiment with C215A and R221A mutant forms of PTP1B. The identity of both mutants was established by sequencing their coding regions as well as the absence of significant catalytic activity (*26*−*28*). Consistent with our current mechanistic proposal, the C215A mutant retained its ability to bind [^{13}C]Cinn-GEE and produced exactly the same three cross-peaks in the HSQC spectrum as the wild-type enzyme (Figure 6). The result with the R221A mutant is more complex. While the three cross-peaks observed with wild-type and C215A PTP1B were clearly absent, we also failed to observe any signal corresponding to the free inhibitor at δ 9.64/201 (data not shown). Careful inspection of the entire spectrum (δ 0−10 for ^{1}H and δ 0−230 for ^{13}C) revealed a single cross-peak of weaker-than-expected intensity at δ 7.2/121. We did notice that upon the addition of Cinn-GEE, a significant fraction of the R221A protein precipitated in the NMR tube, likely causing the weak absorption signal. Our tentative explanation is that the R221A mutant is still capable of binding to Cinn-GEE at high concentrations through noncovalent interactions (500 μM PTP1B and 200 μM Cinn-GEE were used in the NMR experiment). The δ 7.2/121 peak may represent the equilibrium signal from two or more rapidly interconverting species. Thus, the data clearly rule out Cys-215 and are highly suggestive of Arg-221 as the nucleophile responsible for reaction with Cinn-GEE.

To gain further insight into the nature of the Cinn-GEE/Arg adduct (imine vs enamine), we synthesized Cinn-GEE with ^{13}C labeling at the benzylic position (Scheme 3 , compound **17**) and examined its complex with wild-type PTP1B by HSQC experiments. The free inhibitor showed a single cross-peak at δ 7.85/157, consistent with an sp^2 carbon in conjugation with an electron-withdrawing aldehyde (Figure 7A). Addition of excess PTP1B resulted in the disappearance of the free inhibitor signal and the appearance of two new cross-peaks at δ 4.08/47 and δ 4.12/47 positions (Figure 7B). Unfortunately, this region of the spectrum is crowded by many signals of buffer materials. To ascertain that the peaks at δ 4.08/47 and δ 4.12/47 are bona fide signals of the PTP1B/inhibitor complex, a control experiment was performed under exactly the same conditions as in Figure 7B, except that compound **14** was employed. We again observed the three cross-peaks at δ ∼7.7/∼135 (as in Figure 5), but no signal at either the δ 7.85/157 or the δ 4.1/47 region (Figure 7C). The chemical shift values of δ ∼4.1/47 indicate that the benzylic carbon is sp^3-hybridized in the PTP1B/inhibitor complex, suggesting an enamine structure as the enzyme−inhibitor adduct (see Discussion).

There is a slight possibility that the observed inhibitory activity of Cinn-GEE may be due to contamination by a small amount of the more potent cinnamic acid **4** (which could be formed through air oxidation of Cinn-GEE). This notion was tested by treating the inhibitor with excess cysteamine, which reacts with aldehydes to form a stable five-membered thiazolidine ring but should have no effect on the cinnamic acid inhibitor. As expected, prior treatment of Cinn-GEE with excess cysteamine abolished its inhibitory activity against PTP1B (Figure 8). In addition, the cinnamic acid **4** was reported as a simple competitive inhibitor (*20*), whereas the observed inhibition in this work exhibited slow-binding characteristics, consistent with the formation of a reversible enzyme−inhibitor adduct. Taken together, these data rule out the possibility that the observed inhibition was caused by cinnamic acid contamination.

DISCUSSION

Because PTPs play important roles in both physiological and pathological processes, selective inhibitors are expected to provide novel therapeutic agents as well as useful tools for studying their cellular functions. However, despite the great deal of efforts from both academic and industrial laboratories, there have been relatively few reports of truly potent and selective PTP inhibitors (*5*). To date, virtually all of the reported PTP inhibitors contain a negatively charged pY mimetic as the core structure. Such inhibitors suffer from one or both of the following drawbacks. First, the negatively charged pY mimetics often have poor membrane permeability, therefore limiting their applications as therapeutics or research tools in cellular studies. Second, binding of an inhibitor to the PTP active site requires prior desolvation of the inhibitor. For a charged pY mimetic, the cost of desolvation energy can greatly reduce its binding affinity.

We have been pursuing a different approach to PTP inhibitor design. Our strategy is to covalently modify the conserved active-site residues of PTPs using hydrophobic core structures (*29*). Because the catalytic cysteine is

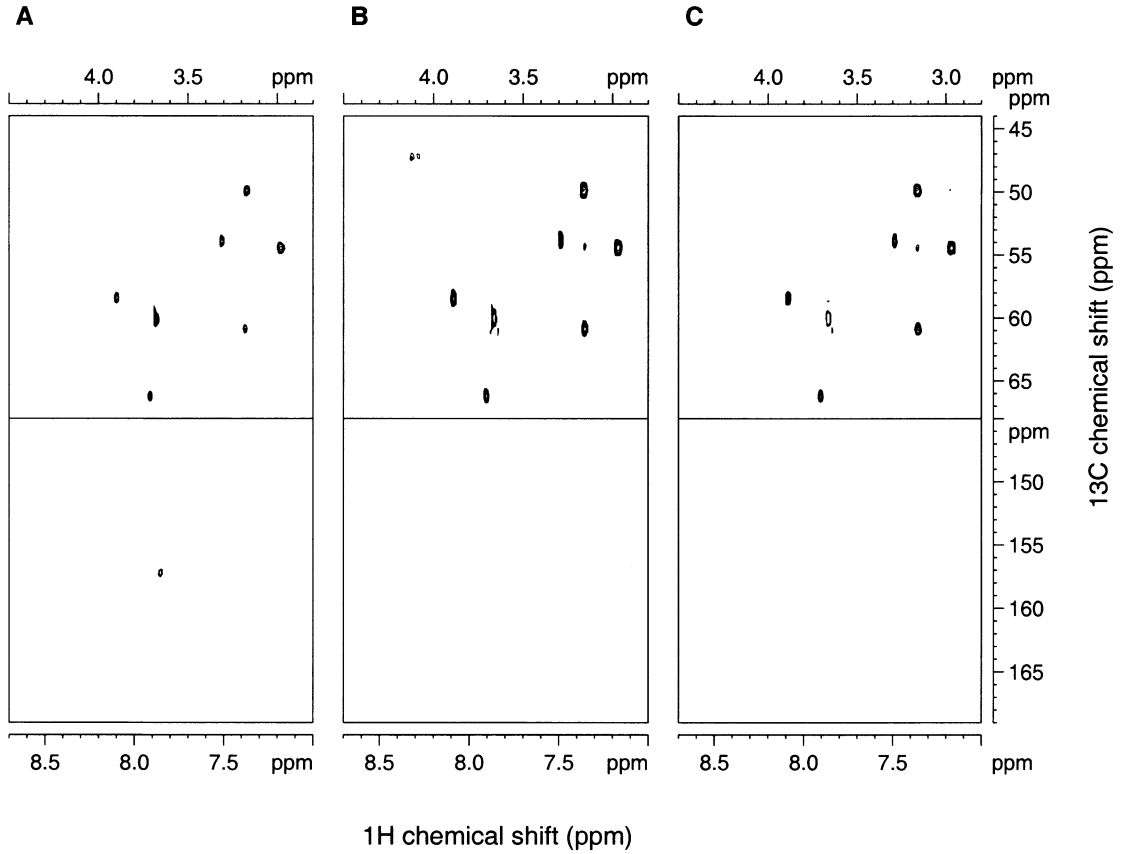

FIGURE 7: HSQC spectra of ^{13}C-labeled Cinn-GEE (compounds **14** and **17**) in the presence and absence of PTP1B. (A) 200 μM inhibitor **17** only; (B) 200 μM inhibitor **17** and 500 μM PTP1B; and (C) 200 μM inhibitor **14** and 500 μM PTP1B.

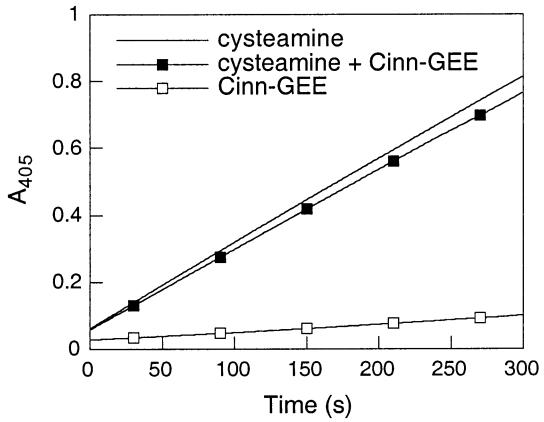

FIGURE 8: Inactivation of Cinn-GEE by cysteamine. PTP1B (0.2 μM) was preincubated with Cinn-GEE alone (20 μM), cysteamine alone (200 μM), or Cinn-GEE (20 μM) and cysteamine (200 μM) before being added to the reaction mixture containing 1.0 mM *p*NPP (pH 7.4).

conserved among all PTPs and is exceptionally acidic (e.g., pK_a = 4.7 in *Yersinia* PTP) (*43*), we reasoned that a peptidyl aldehyde might selectively inhibit PTPs by forming a hemithioacetal adduct with the cysteine thiolate. Since aryl aldehydes are only marginally soluble in water, they should have relatively low desolvation energy, a property that should make them more membrane permeable as well as promote binding to an enzyme active site. In this work, we show that certain aryl-substituted aldehydes indeed act as reversible inhibitors of PTPs. As one might expect from their small sizes, the simple aldehydes do not have high affinity to the PTP active site (IC_{50} values in the high micromolar to millimolar range). However, attachment of a tripeptide GEE to the para position of cinnamaldehyde resulted in an inhibitor of substantially improved affinity to both PTP1B (K_I^* = 5.4 μM) and SHP-1 (K_I^* = 10.7 μM). This suggests that by attaching a properly designed PTP recognition motif or by screening a combinatorial library, one should be able to obtain highly potent and specific inhibitors against a PTP of interest.

Cinn-GEE behaves as a slow-binding inhibitor. Since simple aldehydes (e.g., 4-carboxycinnamaldehyde) exhibit similar slow-binding inhibition, the E·I to E·I* conversion is likely due to structural changes within the active site. Initially, it appeared that the slow-binding behavior could be explained by the time-dependent formation of a reversible hemithioacetal adduct between the aldehyde and the active-site cysteine. Such a mechanism is commonly observed for inhibition of cysteine proteases by peptidyl aldehydes (*43*, *44*). Surprisingly, ^{1}H-^{13}C HSQC experiments with ^{13}C-labeled Cinn-GEE (at the aldehyde carbon) and PTP1B showed three cross-peaks at δ 7.80/130, δ 7.65/132, and δ 7.76/137 positions (Figure 5). These results are inconsistent with the formation of a hemithioacetal, as a hemithioacetal would show no more than two cross-peaks at δ ~5.0 (for the aldehyde-derived ^{1}H) and δ ~85 (^{13}C) (*45*−*47*). The hemithioacetal mechanism is further ruled out by the observation that mutation of the catalytic Cys-215 to alanine had no effect on the HSQC spectrum. The data also rule out the possibility of a free aldehyde (δ 9.64/201) or the hydrate form (which should have a single cross-peak at δ ~5.2/~95) as the bound inhibitor form in the PTP active site.

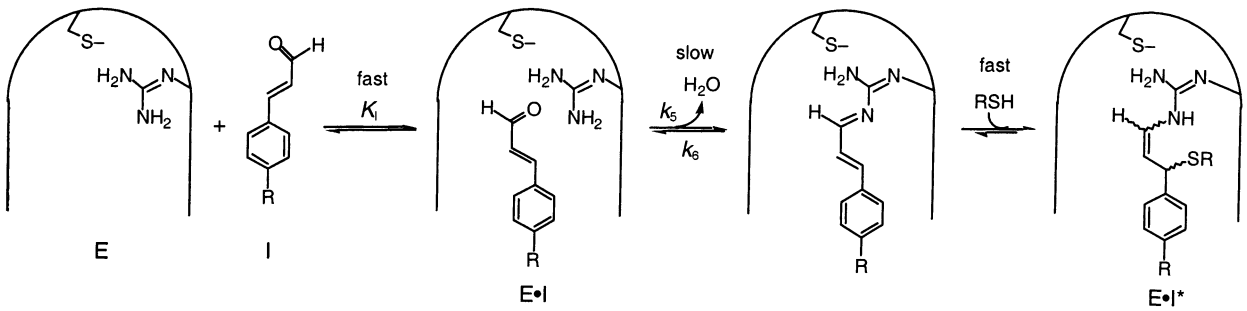

FIGURE 9: Proposed mechanism of inhibition of PTP by cinnamaldehyde derivatives. RSH, β-mercaptoethanol.

We propose that the bound inhibitor forms an enamine adduct with the guanidine group of Arg-221 (Figure 9). Arg-221 is a universally conserved residue present in the PTP signature motif, HCxxGxxR(S/T). It is critical for pY substrate binding and transition-state stabilization by forming a pair of hydrogen bonds between the phosphate nonbridging oxygen atoms and the Nϵ and Nη of Arg-221 (*48*). Binding of the cinnamaldehyde derivatives likely places the carbonyl group at a similar position as the phosphate of a substrate. The close proximity between the aldehyde and the guanidinium group presumably drives the deprotonation of the guanidinium group and the formation of a conjugated imine intermediate. Conjugate addition at the benzylic position by a yet unidentified nucleophile produces the enamine structure as the E·I* complex (Figure 9). This mechanistic proposal is supported by both experiments specifically designed to test the model. First, mutation of Arg-221 to alanine abolished the enamine structure, as evidenced by the absence of the three HSQC cross-peaks observed in wild-type and C215A proteins. Second, HSQC experiment with ^{13}C-labeled Cinn-GEE showed that the chemical shift values for the benzylic proton/carbon decreased from 7.85/157 ppm to ~4.1/47 ppm upon binding to PTP1B. The latter values indicate that the benzylic carbon must be sp^3-hybridized in the E·I* complex, as predicted by our model. The identity of the nucleophile is not yet well established. It may be either a protein side chain (e.g., the second amino group of Arg-221 or Asp-181 which is the general acid/base during catalysis) or a buffer species (e.g., β-mercaptoethanol or a water molecule). The high-field position of the absorption (δ 4.1/47) is most consistent with a thiol being the nucleophile, as the ^{13}C chemical shift values for the benzylic carbon should be well above 60 and 50 ppm when it is directly attached to an oxygen and nitrogen, respectively. The only cysteine near the PTP1B active site is Cys-215, which can be ruled out since its mutation does not affect the enamine structure. Therefore, we propose that the unknown nucleophile is most likely β-mercaptoethanol in the buffer, which was used to maintain PTP1B activity.

Our proposed mechanism also provides a sensible explanation for all of the other experimental observations. Since the formation of enamine is readily reversible, it explains the reversible nature of the inhibitors. Because formation of the imine intermediate requires the expulsion of a water molecule from a relatively deep active site, the reaction is expected to be slow, as is observed. The unknown nucleophile may add from either side of the double bond, and the resulting enamine double bond may assume either a cis or a trans configuration. This can account for the formation of multiple products in the HSQC spectra. Finally, the observed chemical shift values (δ ~132) for the aldehyde-derived carbon atom suggest that this carbon atom is sp^2-hybridized in the E·I* complex. Since the ^{13}C resonance of a typical imine is at δ 150−160, the observed δ values are more consistent with an enamine structure, as predicted by the model. Because we have failed to observe the imine intermediate under any conditions, we propose that conjugate addition by the unknown nucleophile is a rapid step.

In retrospect, the lack of reaction between the aldehyde group and the active-site cysteine of PTPs is not entirely surprising. A nucleophile must approach from above or below the carbonyl plane in order to have a successful addition reaction. Peptidyl aldehyde inhibitors of cysteine proteases are so designed that the aldehyde carbonyl occupies the same position as the amide carbonyl of a scissile bond. Thus, in the E·I complex, the cysteine thiol is properly positioned for nucleophilic attack on the aldehyde. In PTPs, the thiolate is situated at the bottom of the active-site pocket (*48*). This position is ideally suited for a back-attack on an incoming phosphate group, with a collinear S−P−OPh bond angle in the transition state. However, when cinnamaldehyde binds to the PTP active site, the thiolate likely faces the edge of the carbonyl plane. This geometric restriction presumably prevents a successful nucleophilic attack. On the other hand, the Arg-221 side chain is on the wall of the active-site pocket (*48*). This position permits a side attack on the carbonyl plane. Burridge and co-workers have found that calpeptin has modest inhibitory activity against several PTPs but did not examine its mechanism of inhibition (*39*, *40*). Very recently, Urbanek et al. reported a series of 9,10-phenanthrenediones as fairly potent inhibitors of PTP CD45 but not against other PTPs (*49*). On the basis of the slow-binding behavior of the 1,2-diketones, these investigators suggested the formation of a hemithioketal adduct between the inhibitor and the active-site cysteine. In light of the findings in this work, it will be of interest to determine whether calpeptin and the 1,2-diketones also inhibit PTP by covalently modifying the active-site arginine. Note that 1,2-diketo compounds (e.g., phenylglyoxal and 1,2-cyclohexanedione) are commonly used to selectively modify arginine residues in proteins.

In summary, we have demonstrated that certain aryl-substituted aldehydes act as slow-binding inhibitors of PTPs. The time-dependent inhibition is due to the formation of a reversible adduct between the inhibitor and the conserved active-site arginine. These aryl aldehydes and ketones should provide a general core structure that can be further developed into highly potent and specific inhibitors against PTPs.

ACKNOWLEDGMENT

We thank Drs. In-Ja Byeon and Chunhua Yuan of the Campus Chemical Instrument Center (The Ohio State University) for excellent technical assistance in the HSQC NMR experiments, Dr. John Denu for providing the plasmids for overproduction of PTP1B and VHR, and Drs. Ming-Daw Tsai and David Hart for insightful discussions.

REFERENCES

1. Neel, B. G., and Tonks, N. K. (1997) *Curr. Opin. Cell Biol. 9*, 193−204.
2. Hunter, T. (2000) *Cell 100*, 113−127.
3. Zhang, Z.-Y. (2001) *Curr. Opin. Chem. Biol. 5*, 416−423.
4. Elchelby, M., Payette, P., Michaliszyn, E., Cromlish, W., Collins, S., Lee Loy, A., Normandin, D., Cheng, A., Himms-Hagen, J., Chan, C.-C., Ramanchandran, C., Gresser, M. J., Tremblay, M. L., and Kennedy, B. P. (1999) *Science 283*, 1544−1548.
5. Burke, T. R., Jr. and Zhang, Z.-Y. (1998) *Biopolymers 47*, 225−241.
6. Burke, T. R., Jr., Kole, H. K., and Roller, P. P. (1994) *Biochem. Biophys. Res. Commun. 204*, 129−134.
7. Taylor, W. P., Zhang, Z.-Y., and Widlanski, T. S. (1996) *Bioorg. Med. Chem. 4*, 1515−1520.
8. Taylor, S. D., Kotoris, C. C., Dinaut, A. N., Wang, Q., Ramachandran, C., and Huang, Z. (1998) *Bioorg. Med. Chem. 6*, 1457−1468.
9. Taing, M., Keng, Y.-F., Shen, K., Wu, L., Lawrence, D. S., and Zhang, Z.-Y. (1999) *Biochemistry 38*, 3793−3803.
10. Shen, K., Keng, Y.-F., Wu, L., Guo, X.-L., Lawrence, D. S., and Zhang, Z.-Y. (2001) *J. Biol. Chem. 276*, 47311−47319.
11. Ye, B., Akamatsu, M., Shoelson, S. E., Wolf, G., Giogetti-Peraldi, S., Yan, X., Roller, P. P., and Burke, T. R., Jr. (1995) *J. Med. Chem. 38*, 4270−4275.
12. Burke, T. R., Jr., Ye, B., Akamatsu, M., Ford, H., Yan, X. J., Kole, H. K., Wolf, G., Shoelson, S. E., and Roller, P. P. (1996) *J. Med. Chem. 39*, 1021−1027.
13. Akamatsu, M., Roller, P. P., Chen, L., Zhang, Z.-Y., Ye, B., and Burke, T. R., Jr. (1997) *Bioorg. Med. Chem. 5*, 157−163.
14. Roller, P. P., Wu, L., Zhang, Z.-Y., and Burke, T. R., Jr. (1998) *Bioorg. Med. Chem. Lett. 8*, 2149−2150.
15. Sarmiento, M., Wu, L., Keng, Y.-Y., Song, L., Luo, Z., Huang, Z., Wu, G.-Z., Yuan, A. K., and Zhang, Z.-Y. (2000) *J. Med. Chem. 43*, 146−155.
16. Iversen, L. F., Andersen, H. S., Branner, S., Mortensen, S. B., Peters, G. H., Norris, K., Olsen, O. H., Jeppesen, C. B., Lundt, B. F., Ripka, W., Møller, K. B., and Møller, N. P. H. (2000) *J. Biol. Chem. 275*, 10300−10307.
17. Wrobel, J., Li, Z., Sredy, J., Sawicki, D. R., Seestaller, L., and Sullivan, D. (2000) *Bioorg. Med. Chem. Lett. 10*, 1535−1538.
18. Chen, Y. T., Onaran, M. B., Doss, C. J., and Seto, C. T. (2001) *Bioorg. Med. Chem. Lett. 11*, 1935−1938.
19. Malamas, M. S., Sredy, J., Moxham, C., Katz, A., Xu, W. X., McDevitt, R., Adebayo, F. O., Sawicki, D. R., Seestaller, L., Sullivan, D., and Taylor, J. R. (2000) *J. Med. Chem. 43*, 1293−1310.
20. Moran, E. J., Sarshr, S., Cargill, J. E., Shahbaz, M. M., Lio, A., Mjalli, A. M. M., and Armstrong, R. W. (1995) *J. Am. Chem. Soc. 117*, 10787−10788.
21. Cao, X., Moran, E. J., Siev, D., Lio, A., Ohashi, C., and Mjalli, A. M. M. (1995) *Bioorg. Med. Chem. Lett. 5*, 2953−2958.
22. Umezawa, K. (1995) *Adv. Enzyme Regul. 35*, 43−53.
23. Miski, M., Shen, X., Cooper, R., Gillum, A. M., Fisher, D. K., Miller, R. W., and Higgins, T. J. (1995) *Bioorg. Med. Chem. Lett. 5*, 1519−1522.
24. Zhang, Y.-L., Keng, Y.-F., Zhao, Y., Wu, L., and Zhang, Z.-Y. (1998) *J. Biol. Chem. 273*, 12281−12287.
25. Zhang, Z.-Y., and Dixon, J. E. (1994) *Adv. Enzymol. Relat. Areas Mol. Biol. 68*, 1−36.
26. Zhang, Z.-Y., Wang, Y., Wu, L., Fauman, E. B., Stuckey, J. A., Schubert, H. L., Saper, M. A., and Dixon, J. E. (1994) *Biochemistry 33*, 15266−15270.
27. Guan, K. L., and Dixon, J. E. (1990) *Science 249*, 553−556.
28. Pot, D. A., and Dixon, J. E. (1992) *J. Biol. Chem. 267*, 140−143.
29. Arabaci, G., Guo, X.-C., Beebe, K. D., Coggeshall, K. M., and Pei, D. (1999) *J. Am. Chem. Soc. 121*, 5085−5086.
30. Pei, D., Neel, B. G., and Walsh, C. T. (1993) *Proc. Natl. Acad. Sci. U.S.A. 91*, 1092−1096.
31. Puius, Y. A., Zhao, Y., Sullivan, M., Lawrence, D. S., Almo, S. C., and Zhang, Z.-Y. (1997) *Proc. Natl. Acad. Sci. U.S.A. 94*, 13420−13425.
32. Denu, J. M., Zhou, G., Wu, L., Zhao, R., Yuvaniyama, J., Saper, M. A., and Dixon, J. E. (1995) *J. Biol. Chem. 270*, 3796−3803.
33. Daubresse, N., Francesch, C., and Rolando, C. (1998) *Tetrahedron 54*, 10761−10770.
34. Lu, T.-J., Yang, J.-F., and Sheu, L.-J. (1995) *J. Org. Chem. 60*, 2931−2934.
35. Freer, D., and Morecombe, D. J. (1992) *J. Labeled Compd. Radiopharm. 16*, 695−710.
36. Vuister, G. W., and Bax, A. (1992) *J. Magn. Reson. 98*, 428−435.
37. Schedletzky, O., Glaser, S. J., Sorensen, O. W., and Griesinger, C. (1994) *J. Biomol. NMR 4*, 301−306.
38. Veber, D. F., and Thompson, S. K. (2000) *Curr. Opin. Drug Discovery Dev. 3*, 362−369.
39. Schoenwaelder, S. M., and Burridge, K. (1999) *J. Biol. Chem. 274*, 14359−14367.
40. Schoenwaelder, S. M., Petch, L. A., Williamson, D., Shen, R., Feng, G.-S., and Burridge, K. (2000) *Curr. Biol. 10*, 1523−1526.
41. Yuvaniyama, J., Denu, J. M., Dixon, J. E., and Saper, M. A. (1996) *Science 272*, 1328−1331.
42. Morrison, J. F., and Walsh, C. T. (1988) *Adv. Enzymol. Relat. Areas Mol. Biol. 61*, 201−301.
43. Zhang, Z.-Y., and Dixon, J. E. (1993) *Biochemistry 32*, 9340−9345.
44. Lewis, C. A., Jr., and Wolfenden, R. (1977) *Biochemistry 16*, 4890−4894.
45. Bendall, M. R., Cartwright, I. L., Clark, P. I., Lowe, G., and Nurse, D. (1977) *Eur. J. Biochem. 79*, 201−209.
46. Zhou, M., and Van Etten, R. L. (1999) *Biochemistry 38*, 2636−2646.
47. Sundaramoorthi, R., Siedem, C., Vu, C. B., Dalgarno, D. C., Laird, E. C., Botfield, M. C., Combs, A. B., Adams, S. E., Yuan, R. W., Weigele, M., and Narula, S. S. (2001) *Bioorg. Med. Chem. Lett. 11*, 1665−1669.
48. Jia, Z., Barford, D., Flint, A. J., and Tonks, N. K. (1995) *Science 268*, 1754−1758.
49. Urbanek, R. A., Suchard, S. J., Steelman, G. B., Knappenberger, K. S., Sygowski, L. A., Veale, C. A., and Chapdelaine, M. J. (2001) *J. Med. Chem. 44*, 1777−1793.

BI0258748